

EFFECT OF CO₂ LEAKAGES ON AUTOTROPHIC GROWTH IN THE
SUBSURFACE DURING GEOLOGICAL SEQUESTRATION

by

Nichole Michelle Comber

A thesis submitted to the faculty of
The University of Utah
in partial fulfillment of the requirements for the degree of

Master of Science

Department of Civil and Environmental Engineering

The University of Utah

August 2012

Copyright © Nichole Michelle Comber 2012

All Rights Reserved

THE UNIVERSITY OF UTAH GRADUATE SCHOOL

STATEMENT OF THESIS APPROVAL

The thesis submitted by Nichole Michelle Comber
has been approved by the following supervisory committee members:

<u>Ramesh K. Goel</u> ,	Chair	<u>5/11/2012</u> Date Approved
<u>Brian J. McPherson</u> ,	Member	<u>5/11/2012</u> Date Approved
<u>Otakuye Conroy-Ben</u> ,	Member	<u>5/11/2012</u> Date Approved

and by Paul J. Tikalsky, Chair of
the Department of Civil and Environmental Engineering

and by Charles A Wight, Dean of The Graduate School.

ABSTRACT

In recent years, the release of carbon dioxide into the atmosphere has been a growing concern. In order to mitigate this problem, technological options to help stabilize the CO₂ concentrations have been studied by scientists all over the world. One of the more promising solutions, called geological sequestration, is comprised of pumping captured CO₂ underground and storing it in deep saline aquifers. However, long-term storage CO₂ raises concerns, the most prominent being the effect of the carbon dioxide if it were to escape.

Batch reactors were set up to determine the effect of carbon dioxide on the aerobic bacterium *Nitrosospria multiformis* and the anaerobic archaeon *Methanobacterium subterraneum*. The *N. multiformis* was grown over a period of 5 days. Live and dead cells were enumerated using a BacLight kit and an epifluorescence microscope. The *M. subterraneum* was grown over a period of 6 days and enumerated using Flow-FISH (Flourescent In Situ Hybridization) with a MB1174 probe and DAPI. It was determined that both autotrophic growths were supported by carbon dioxide gas. The aerobic autotrophic bacterium *N. multiformis* had more growth when supplied with bicarbonate as a carbon source, but the CO₂ had no inhibitory effects. The anaerobic archaeon *M. Subterraneum* growth was stimulated by the addition of CO₂ gas. Optimization of this protocol would give more accurate results, but since little research has been conducted on the effect of geologic carbon sequestration on deep subsurface microbiology, this study laid down an important foundation for future research.

TABLE OF CONTENTS

ABSTRACT	iii
LIST OF FIGURES	v
ACKNOWLEDGMENTS	vi
CHAPTER	
1. INTRODUCTION	1
2. OBJECTIVES AND TASKS	5
Expected Outcome	6
3. BACKGROUND INFORMATION	7
CO ₂ Sequestration Concerns	8
CO ₂ in Groundwater	10
CO ₂ Effect on Geochemistry	14
CO ₂ Effect on Microbiology	15
4. MATERIALS AND METHODS	22
Task 1- Initialize Autotrophic Growth	22
Task 2- Setup Experiment	27
Task 3- Quantify and Analyze Autotrophic Growth	31
5. RESULTS AND DISCUSSION	35
Experiments with Aerobic Autotrophic Bacteria	35
Experiments with Anaerobic Autotrophic Archaea	40
6. CONCLUSIONS	48
REFERENCES	50

LIST OF FIGURES

<u>Figure</u>	<u>Page</u>
1- Geologic sequestration of CO ₂ and its fate if leakage occurs.....	2
2- Scheme of subterranean microbial anaerobic community based on energy of hydrogen (Kotelnikova, 2002).....	18
3- Batch reactor experimental setup for aerobic autotrophs.....	28
4- Experimental setup for anaerobic autotrophs	30
5- Epifluorescent <i>N. multiformis</i> stained with BacLight	36
6- Cell counts in terms of dead, live, and total cell numbers for <i>N. Multiformis</i> which received inorganic carbon source in the form of A) CO ₂ gas B) bicarbonate C) CO ₂ gas and bicarbonate	37
7- Partial nitrification performed by <i>N. multiformis</i> with inorganic carbon in the form of A) just CO ₂ gas B) just bicarbonate C) both bicarbonate and CO ₂ gas.....	39
8- <i>M. Subterraneum</i> viewed under epifluorescent microscopy comparing a Cy3 probe (top) to DAPI staining (bottom)	42
9- Flow cytometry forward scatter for reactor 1.....	43
10- Enumerated cells through flow cytometry	44
11- Flow cytometry enumeration for <i>M. Subterraneum</i> stained by A) DAPI and B) Cy3 probe.....	45
12- Enumeration of <i>M. subterraneum</i> stained with A) DAPI and B) Cy3 probe normalized based on initial concentrations	46

ACKNOWLEDGMENTS

It is a pleasure to thank many people who made this thesis and research possible, including the support I received from my advisor, Dr. Ramesh Goel, who gave me the opportunity and training by working in his laboratory and who helped me develop the objectives of the task. I wish to thank professor Dr. Brian McPherson for including me in the overall project for EPA and helping fund the experiment. The quality of this experiment was greatly enhanced by the gracious assistance of Shireen Meher Kotay, who helped guide the experiment and instructed me on different analysis methods. I also would like to thank James Marvin and the CORE facility for running the flow cytometer and helping with analysis. Lastly, I would like to thank my lab-mates, my parents, and my close friends, who constantly offered me support and encouragement. Without that support, it would have been difficult to accomplish this work.

CHAPTER 1

INTRODUCTION

The past few decades, global warming due to green house gas emissions has been an issue that has stimulated much discussion among environmentalists. In its 2007 scientific report, the Intergovernmental Panel on Climate Change (IPCC) presented new and stronger evidence that most of the warming observed over the past 50 years is attributed to human influences. These influences are expected to continue to change atmospheric conditions throughout the next century (IPCC, 2007). The largest human induced contributor to green house gases is carbon dioxide, CO₂. Atmospheric CO₂ has increased by almost 100 ppm since preindustrial levels with increasing annual growth rates (IPCC, 2007). Technological options to help stabilize the CO₂ concentrations have been studied by scientists all over the world. A few of these include: reducing energy consumption, switching to less carbon intensive fuels, increasing the use of renewable energy sources, and sequestering CO₂ by enhancing biological absorption capacity in forests and soils. In a special report, IPCC identified capturing and storing CO₂ as having the potential to effect climate change. Carbon dioxide capture and storage has several different options, including ocean storage and mineral carbonation, but the most viable option is its geological sequestration (IPCC, 2005).

In geologic sequestration (Figure 1), carbon dioxide is captured and injected into deep saline aquifers for long-term storage. These saline aquifers contain highly mineralized brines that have been considered of no benefit to humans. The carbon dioxide that is pumped underground has sufficient high pressure (greater than 7.38 MPa) and temperature (greater than 31.1°C) to be in a supercritical state, meaning it is above the critical point and fills a container like a gas, but has a density like that of a liquid. The depth of the injection is expected to have the required pressure and temperature needed to maintain the CO₂ in a supercritical state. However, even if CO₂ is kept as a supercritical fluid, the CO₂ injected in sedimentary basins will always be more buoyant than the underlying formation water. Therefore, once injected, the CO₂ will rise to the top of saline formations and be trapped by a cap rock.

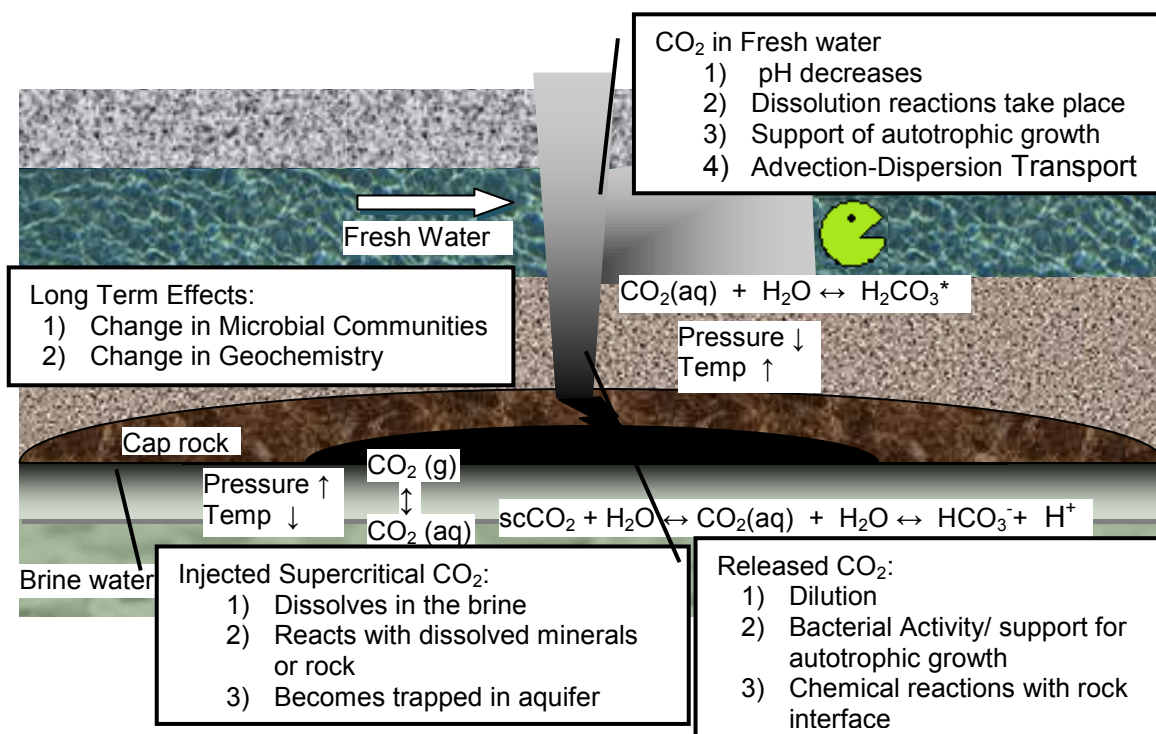


Figure 1- Geologic sequestration of CO₂ and its fate if leakage occurs

Since initial deep injection of CO₂ is likely to occur in mature basins using existing infrastructure, possible leakage through existing wells or weakened cap rock integrity needs to be considered. Also, since subterranean geological infrastructure is largely unknown, CO₂ may degrade the cap rock minerals over time, creating cracks that allow the CO₂ to escape, as seen in Figure 1. With the release of the pressure built up under the cap rock, the supercritical CO₂ may be released as liquid and gaseous CO₂. Gaseous and liquid CO₂ react more readily with the subsurface geochemistry and autotrophic bacteria that already exist in the system can use it as a new carbon source.

As it rises, the CO₂ is dissolved into the fresh water aquifer. Carbon dioxide is soluble in water, depending upon the pH of water. Over the ordinary temperature range, the solubility in water is about 200 times that of oxygen. Calcium and magnesium combine with carbon dioxide to form carbonates and bicarbonates. When CO₂ dissolves, it shares the physical properties of the substrate and no longer behaves independently (IPCC, 2005). Therefore, it begins to travel by advection and dispersion within the ground water. Excess CO₂ in the groundwater could cause a drop in pH. This lower pH could cause dissolution of other rock formations into the system. Any microbiology in the water down flow from the leakage site could be affected.

Hence, there are two major issues if the sequestered CO₂ leaks and travels to upper strata depending upon the cap rock integrity and these issues are:

(1) CO₂ can change the system pH, thus initiating changes in geochemistry.

(2) The subsurface and water microbiology can be affected directly by CO₂ because CO₂ can serve as a carbon source for the autotrophic bacteria.

Both these issues are important but my research primarily focused on the second issue which is the effect of CO₂ on autotrophic microorganisms residing in the subsurface. My specific research objectives, a detailed literature review, materials and methods, results and discussion, and conclusions are presented later in this thesis in the given order.

CHAPTER 2

OBJECTIVES AND TASKS

Inorganic sources of carbon only effect chemolitho-autotrophic bacteria which consume carbon dioxide. In deep strata, anoxic conditions are prevalent. Under oxygen free conditions, presumably only anaerobes will be affected. On the other hand, ground water is not strictly anaerobic. Wells, cracks, and other variables can introduce oxygen into the system which can create scenarios that could cause aerobes to be affected. Under these assumptions, the following objectives were created:

1. Study CO₂ effect on growth rate of aerobic autotrophs. Nitrifiers will be used as a classical example because they are found everywhere, including soil. For this purpose, the aerobic autotrophic *Nitrosospira multiformis* (ATCC 25196) was selected as a model organism.
2. Study CO₂ effect on the growth rate of anaerobic autotrophs. Methanogens will be used as an example because of their known presence in the deep subsurface. As a model organism, the strictly anaerobic archaeon *Methanobacterium subterraneum* (ATCC 700657) was selected.

To accomplish the objectives, the following plan was created.

1. Task 1- Initialize autotrophic growth
 - 1.1 Growth of aerobic autotrophs

- 1.2 Growth of anaerobic autotrophs
- 2. Task 2- Setup experiment
 - 2.1 Experimental setup to study growth of aerobic autotrophs
 - 2.2 Experimental setup to study the growth of anaerobic autotrophs
- 3. Task 3- Quantify and analyze autotrophic growth

Expected Outcome

Although the research does not involve contamination transport involving bacterial growth rates, the growth rate constant obtained through experimentation can be utilized in modeling practices targeting CO₂ fate and transport.

CHAPTER 3

BACKGROUND INFORMATION

Of all the green house gases, CO₂ is responsible for about 64% of the enhanced 'greenhouse effect,' making it the target for mitigation of greenhouse gases (Bachu and Adams, 2003). Carbon dioxide capture and sequestration (CCS) has recently come to play as a viable option to reduce atmospheric concentrations of CO₂ in order to help minimize the effect of greenhouse emissions on the climate. Carbon sequestration means putting carbon dioxide somewhere other than into the atmosphere. If CCS is implemented on the scale needed to make noticeable reductions in atmospheric CO₂, a billion metric tons or more must be sequestered annually (Benson and Cloe, 2008).

Although there are several options for carbon sequestration, including ocean storage and mineral carbonation, geologic sequestration has been identified as the most technically viable option (IPCC, 2005). Geological sequestration happens when carbon dioxide is injected at supercritical fluid conditions into deep saline aquifers or abandoned oil/gas wells for long-term storage. Geological sequestration is a means of reducing anthropogenic atmospheric emissions of CO₂ that is immediately available and technologically feasible. Among various options, CO₂ can be sequestered in deep aquifers by dissolution in the formation water. The ultimate CO₂ sequestration capacity in solution (UCSCS) of an aquifer is the difference between the total capacity for

CO₂ at saturation and the total inorganic carbon currently in solution in that aquifer, and depends on the pressure, temperature, and salinity of the formation water (Bachu and Adams, 2003). As stated by the Intergovernmental Panel on Climate Change: "For well-selected, designed and managed geological storage sites, the vast majority of the CO₂ will gradually be immobilized by various trapping mechanisms and, in that case, could be retained for up to millions of years." It has been estimated that the United States has available storage capacity from 1,300 to 3,900 gigatons of carbon dioxide, the majority of which is in deep saline formations (NETL, 2007). For reference, the total energy-related CO₂ emissions in the United States in 2005 was 5.9 gigatons, with fossil fuel combustion accounting for 5.8 gigatons (U.S. EPA, 2008).

CO₂ Sequestration Concerns

CO₂ sequestration poses several concerns to local and global biology and ecology. The primary threat is due to CO₂ leakage from an underground well. Typical concentrations of CO₂ in soils are 0.2-4% (Benson et al., 2002), but vary with depth, time of year, soil type, and water content. Concentrations of 20-30% were found to be sufficient to alter characteristics of entire ecosystems. For example, though plants need CO₂ for photosynthesis and high levels of the gas can enhance a plants growth, CO₂ concentrations at Mammoth Mountain, California of 30% caused the death of all trees in the affected area, regardless of type or age (Saripalli et al., 2002).

The gas also poses a threat to ground dwelling animals (burrowers, ground dwelling birds, and many reptiles) especially those whose physiology

makes them sensitive to high concentrations of CO₂. Though the effects of CO₂ tolerances on vertebrates other than humans have not been extensively studied, research shows that concentrations of 40% cause behavioral changes and paralysis in birds. Additionally, many surface dwelling animals depend on surface vegetation, which can be affected as discussed above.

Changes in pH as a result of high concentrations of CO₂ also negatively affect marine life and corals. These animals have been shown to be highly susceptible to small changes in pH as the acidification may cause them to lose the ability to form shells or corals (Turley et al., 2006).

There are also concerns about the quality of ground water when exposed to high concentrations of CO₂ gas. The gas has the potential, depending on the chemistry of the aquifer, to effect the salinity, acidity, and enable the mobilization of heavy metals and other impurities because of pH changes (U.S. EPA, 2008). Strict regulations and tolerances are put in place by the EPA to regulate the amount of TDS and metals allowed in drinking water, but very little research exists to actually quantify the effects of CO₂ interactions with aquifers. These effects are difficult to quantify because of the great variability in geochemistry, microbial presences, and natural buffering capacity from aquifer to aquifer.

Leakage

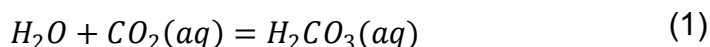
Leakage from the CO₂ sequestration site is the primary source of concern for environmentalists, but it is also of primary importance to those designing such a system. There are a number of ways for a CO₂ reservoir to leak, i.e., natural fissures in the earth, faults, man-made cracks in the crust caused by over

pressurizing a well, and diffusion of CO₂ through rock or other porous media. All of these things are collectively referred to as “cap-rock failure.” This leakage has the potential to reduce the viability of underground CO₂ sequestration as an effective mitigation option.

Given that all pressurized underground wells leak in some capacity, the question for the industry has been to determine what leakage rates are acceptable and will ensure the stabilization of atmospheric CO₂. Research has shown that there is a range of acceptable leakage rates, but that it is generally accepted that 0.1% per year is the maximum allowable leakage rate (Damen, 2006).

CO₂ in Groundwater

If leakage occurs, the CO₂ will move upwards, driven by buoyance, and may reach overlaying aquifers, where it will dissolve into the shallow groundwater. Carbon dioxide occurs naturally in groundwater as the result of respiration in soil that dissolves in water and is not degassed out of the soil into the air (Cole and Prairie, 2009), and a small amount of CO₂ added to the system will cause little risks by itself. Total dissolved inorganic carbon content in the groundwater is made up of bicarbonate ion (HCO₃⁻), the carbonate ion (CO₃²⁻), and aqueous carbon dioxide, which consists of two pools (dissolved free CO₂ and its hydrated form H₂CO₃) since CO₂ is not a charged species and interchanges readily with H₂CO₃.



The pH can help determine how much of each constituent there is relative to each other. In natural waters at pH less than 5.3, only CO_2 is found; as the pH increases, HCO_3^- will form and CO_2 will diminish. CO_2 and HCO_3^- are in equal quantities at pH 6.3 (Cole and Prairie, 2009); after that point, HCO_3^- will be dominant as the CO_2 diminishes and CO_3^{2-} begins to be introduced. At pH 10.3, CO_3^{2-} becomes dominant and HCO_3^- diminishes.

The transfer of dissolved CO_2 to groundwater is expressed as the mass transfer coefficient, K_L . The transfer flux from gas to liquid can be obtained from the relationship between the concentration gradient and diffusive flux or the transfer of substances from the gas phase into a liquid:

$$F = K_L \left[\frac{C_g}{H} - C_l \right] \quad (2)$$

where F = Diffusive flux across a gas-liquid interface ($\text{mass m}^{-2}\text{h}^{-1}$)

C_g = Concentration of substance in the liquid phase (mass m^{-3})

C_l = Concentration of the substance in the liquid phase (mass m^{-3})

H = Henry's Law coefficient (dimensionless)

Due to the nature of the capillary fringe, located just above the water table, the K_L cannot be calculated and it has to be obtained experimentally. However, it has an upper bound value of $1.3 \times 10^{-4} \text{ cm/s}$ for an open-air CO_2 gas transfer to quiescent water under ambient room conditions. The mass transfer of gases to groundwater is a complex process that is difficult to predict, partially due to porous media, capillary fringe, and the fine boundary between saturated and unsaturated soil (Caron et al., 1998). Carbonated water is not directly detrimental

to drinking water, but too much CO₂ causes secondary effects caused by the increased CO₂ dissolution into the system and can be considered a contaminant.

Groundwater Flow and Contaminant Transport

Once dissolved, the CO₂, like other contaminants that are dissolved, called solutes, is transported with the water as it flows. Flow of groundwater in the subsurface is complex and assumptions to simplify are necessary. A porous media model is often used to quantify the nature of the subsurface. Porosity is defined as a dimensionless ratio between the volume of the void to the total volume (LaGrega et al., 2010). The effective porosity, the ratio of pore volume containing flowing volume to bulk volume of the sand, is viewed as the porosity required in order to achieve agreement with observation in a calculation of travel time (Zheng and Bennet, 1995). Darcy's law is the fundamental relation describing flow in porous media. Darcy's law is empirical and has been verified by subsequent experiments over a wide range of flow conditions. It is valid as long as the flow is laminar (LaGrega et al., 2010). His findings are presented in algebraic form:

$$V_D = \frac{Q}{A} = ki \quad (3)$$

where V_D = Darcy's velocity

Q = flow rate $\left(\frac{cm^3}{s}\right)$

A = cross-sectional area of flow perpendicular to the direction (cm^2)

k = hydraulic conductivity $\left(\frac{cm}{s}\right)$

i = hydraulic gradient $\left(\frac{cm}{cm}\right)$

Darcy velocity, or specific discharge, is not the seepage velocity since it assumes that flow occurs across the entire cross-section of the soil sample. Flow actually takes place only through interconnected pore channels. Seepage velocity, or interstitial velocity, is the movement of the water through the porous medium. The seepage velocity is always faster than the Darcy velocity.

$$V_S = \frac{V_D}{n} \quad (4)$$

where $V_S = \text{Seepage velocity}$
 $V_D = \text{Darcy's velocity}$
 $n = \text{Porosity}$

Seepage velocity can also be estimated from the observed travel time of a tracer (Zheng and Bennet, 1995).

When solutes are transported along stream lines at the average linear seepage flow velocity, it is termed advection. The porous medium model governs the flow rate and direction of the contaminant; however, as the water flows around solids, the contaminant is mixed with the flowing water (LaGrega et al., 2010). Dispersive transport, or hydrodynamic dispersion, addresses the effects of the individual particle as it deviates from the average seepage velocity. The most important effect of dispersion is to spread the contaminant mass beyond the region it would occupy otherwise (Zheng and Bennet, 1995). The result is a dilution or reduction in contaminant concentration. Thus, contaminants are transported by advection and their concentrations change as a result of dispersion (LaGrega et al., 2010).

From Darcy's Law, a 3-D equation for contaminant flow can be derived. For an incompressible fluid, isotropic, homogeneous medium, the flow is found using the Laplace Equation:

$$\frac{\partial^2 h}{\partial x^2} + \frac{\partial^2 h}{\partial y^2} + \frac{\partial^2 h}{\partial z^2} = 0 \quad (5)$$

CO₂ Effect on Geochemistry

As dissolved CO₂ flows with the shallow groundwater, it affects the entire geochemical balance as it comes in contact with the parent rock material. CO₂ is the major chemical responsible for the dissolution of rocks, particularly carbonate rocks and aluminosilicate minerals. However, if a contaminated system comes in contact with solid carbonate, such as limestone, the CO₂ will be consumed in the dissolution of carbonate, forming more HCO₃⁻ (Cole and Prairie, 2009). These reactions convert dissolved CO₂ into carbonate and bicarbonate, which is the main source of alkalinity. The following equations show how carbonate, pH, and alkalinity are related:

$$\text{Alkalinity} = C_T(\alpha_1 + 2\alpha_2) + \frac{K_W}{[H^+]} + [H^+] \quad (6)$$

where K_W = dissociation constant of water,
 C_T = the total carbonate in the system,

$$C_T = [H_2CO_3^*] + [HCO_3^-] + [CO_3^{2-}] \quad (7)$$

$$[H_2CO_3^*] = C_T \alpha_0 \quad (8)$$

$$\alpha_0 = \left[1 + \frac{K_1}{[H^+]} + \frac{K_1 K_2}{[H^+]^2} \right]^{-1} \quad (9)$$

$$\alpha_1 = \left[1 + \frac{[H^+]}{K_1} + \frac{K_2}{[H^+]} \right]^{-1} \quad (10)$$

$$\alpha_2 = \left[1 + \frac{[H^+]}{K_2} + \frac{[H^+]^2}{K_1 K_2} \right]^{-1} \quad (11)$$

K_1 and K_2 are temperature-dependent and express the ratios between the carbonate species. At 20°C, $K_1 = 10^{-6.38}$, and $K_2 = 10^{-10.377}$. Unless $\text{pH} \gg 7.5$, K_2 can be ignored.

CO_2 affects pH because:

$$[H^+] = \frac{K_1[CO_2]}{[HCO_3^-]} \quad (12)$$

If CO_2 increases, $[H^+]$ increases and pH goes down, becoming more acidic (Stumm and Morgan, 1995). Such acidic conditions can affect the dissolution and sorption mechanisms of many minerals, especially calcite and iron oxyhydroxides. Some trace metals also will experience desorption due to a decrease in pH (Wang and Jaffe, 2004).

CO_2 Effect on Microbiology

Along with affecting the geochemistry, it is possible for the addition of CO_2 to affect the subsurface microbiology since the addition of carbon dioxide into a closed system adds an additional carbon source that was not originally there. Microbes are also affected by the dissolution of the minerals in complex biochemical reactions.

Carbon and energy sources, usually referred to as substrates, are necessary for cell growth. Carbon can be obtained from organic matter or carbon dioxide. Microorganisms that use organic carbon for new biomass are called *heterotrophs*. *Autotrophs* use inorganic carbon, such as carbon dioxide,

as a carbon source. Energy for cell synthesis may be supplied by light or a chemical oxidation reaction. *Phototrophs* use light as an energy source while *chemotrophs* derive their energy from a chemical reaction. Phototrophs and chemotrophs can be either autotrophic or heterotrophic. For example, *Chemoautotrophs*, such as nitrifying bacteria, utilize CO₂ as a carbon source and obtain energy from the oxidation of inorganic compounds (Metcalf & Eddy, Inc., 2003).

Owing to their immense physical, chemical, and biological heterogeneity, soils are considered the most microbially diverse environments on earth. Environmental factors that influence microbial community composition and diversity include pH, particle size, organic carbon, nutrient availability, water content, and oxygen concentration. The abundance, composition, and diversity of microbial communities within soil are strongly depth-dependent. The top 7 cm contain the highest concentration and greatest diversity of bacteria. The soil area deeper around the roots of plants and trees contain a concentrated amount of nitrifying bacteria, such as *Nitrosolobus*, *Nitrospina*, and *Cyanobacteria*. In these depths, aerobic bacteria are dominant. As soil depth increases, bacterial content and diversity decrease as temperature, oxygen levels, and organic matter decrease. Anaerobic bacteria dominate these soils. Interestingly, while numbers of bacteria were consistently higher than those of archaea, the ratio of archaeal genes increases with soil depth (Hansel et al., 2008).

Deep Subsurface Microbiology

Deep geologic ecosystems support significant communities of microbial life but are poorly characterized. Microbial life is ubiquitous and extends several miles into the Earth's crust (as deep as 4,000 meters), and in all of the types of locations being considered for geologic sequestration (IPCC, 2005; U.S. EPA, 2008). At these extreme depths, the microbes catalyze reactions using compounds such as CO₂ to derive energy. In CO₂ sequestration, carbon dioxide leakage could affect these organisms. However, since few experiments have been conducted in the area, the effect on microorganisms in soil due to a change in CO₂ is largely unknown at extreme depths (U.S. EPA, 2008; Benson et al., 2002). Various studies and research projects have been conducted on the impact of pH decrease on CO₂ injection in the ocean or marine ecosystems. However, there is a large difference of the ecosystem in the ocean compared to the one created in deep geologic formations (Damen, 2006).

Deep subsurface microbiology consists mostly of four anaerobic, physiological types: methanogens, sulfate reducing bacteria, fermentative anaerobes, and iron reducing bacteria (Onstott, 2005). Figure 2 shows the subterranean anaerobic communities. The two types that can directly utilize CO₂ as a carbon source are acetogens and methanogens.

The reduction of pH is the most readily identified impact of CO₂ injections on the subsurface microbial communities. Microbial Fe(III) reduction reactions are particularly more significant since Fe(III)-bearing oxides and electron donors are usually present in aquifers. The effect on the microbes will differ depending

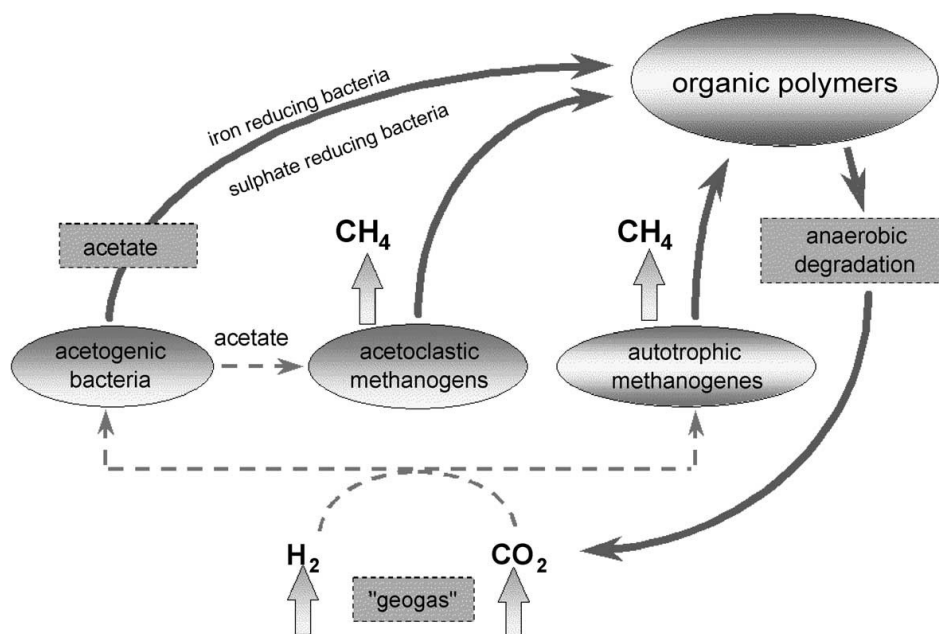
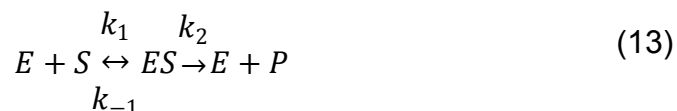


Figure 2-Scheme of subterranean microbial anaerobic community based on energy of hydrogen (Kotelnikova, 2002)

on the geochemistry of the region. For example, long-term storage of CO₂ in silicastic reservoirs will allow Fe(III)-reducing microorganisms to increase the pH and lead to the precipitation of various carbonates. As the Fe(III) is depleted and sulfate is not a major constituent in the ground water, then methanogenic activity will begin to dominate based on the CO₂/H₂ ratios (Onstott, 2005). On the other hand, a dolomitic or carbonate aquifer will not have the same buffer and the dissolution of the carbonate will not restore the pH to a range that allows the growth of some microorganisms. If mafic igneous rock is present and contains Fe, then the lower pH will allow the release of H₂ and oxidize ferrous iron to Fe(OH)₃. This allows methanogenic and acetogenic communities to be stimulated. Fe(III)-reducing bacteria could be stimulated by Fe(OH)₃ leading to Fe(III) reduction and a rise in pH (Onstott, 2005).

Bacterial Growth Kinetics

A mathematical model of the kinetics of a single-substrate-enzyme-catalyzed reaction was first developed by V.C.R. Henri in 1902 and by L. Michaelis and M. L. Menten in 1913. It is referred to as Michaelis-Menten kinetics or saturation kinetics (Shuler and Kargi, 2002). The simple reaction scheme shows the saturation kinetics, with a reversible step for enzyme-substrate complex formation and a dissociation step of the ES complex into the enzyme and the product.



When applied to cellular systems, the relationship of specific growth rate to substrate concentration often assumes the form of saturation kinetics. Under substrate limited growth, this is described by the Monod equation:

$$\mu_g = \frac{\mu_m S}{K_s + S} \quad (14)$$

where μ_m = maximum specific growth rate when $S \gg K_s$

S = substrate

K_s = saturation constant or half velocity constant

If endogenous metabolism is unimportant, $\mu_g = \mu_{net}$. In general, $\mu_g = \mu_m$ for $S \gg K_s$.

The Monod equation is semiempirical since it is derived from the Michaelis-Menten kinetics premise for the uptake of S , and the amount of that

enzyme is growth-rate limiting. However, it fits a wide range of data satisfactorily (Shuler and Kargi, 2002).

The Michaelis-Menten equations are based on data from batch reactors. In a batch reactor, there are typically five different phases in the growth phase.

- 1) Lag phase: happens immediately after inoculation and represents the time required for bacteria to acclimate to their new environment.
- 2) Logarithmic or exponential-growth phase: bacteria are not limited due to substrate or nutrients and multiply at their maximum rate and cell number increases exponentially with time. All components grow at the same rate, which can be determined from cell number. The growth rate is first-order and independent of nutrient concentration:

$$\frac{dX}{dt} = \mu_{net} X \quad (15)$$

$$\ln \frac{X}{X_0} = \mu_{net} t \quad (16)$$

$$\mu_{net} = \frac{\ln X_2 - \ln X_1}{t_2 - t_1} \quad (17)$$

where, μ_{net} = maximum net specific growth rate
 X = cell concentration ($\frac{g}{L}$)

- 3) Deceleration growth phase: growth decelerates due to depletion of nutrients or accumulation of toxic by-products of growth. This is short and allows unbalanced growth.
- 4) Stationary phase: net growth rate is zero or equal to the death rate.
- 5) Death phase: Nutrient depletion or toxic product accumulation causes cells to die. The rate of death follows first-order kinetics.

The interconnection between microbiology and geochemistry is complex and site-specific. Much of the research done for geologic sequestration leakage has focused on the effect of CO₂ on the geochemistry, while little is known about its effects on the microbiology and the effect those microorganisms play in the overall biogeochemistry. The research that was conducted in this thesis emphasized carbon dioxide's effect on microbiology and its growth rate independent of the geochemistry changes.

CHAPTER 4

MATERIALS AND METHODS

Task 1- Initialize Autotrophic Growth

Autotrophic bacteria require an inorganic carbon source and will convert it to an organic form during their metabolism. To investigate the effect of CO₂, two physiologically different microorganisms were chosen: an aerobic bacterium and an anaerobic archaeon. Autotrophic microbes are extremely slow growers due to the energetically poor substrates they metabolize. Hence, a great deal of time was needed to obtain and maintain a measurable population. Furthermore, the optimum growth conditions (viz., temperature, aerobicity/anaerobicity, pH) for the microbes were stringent, which required significant time towards method development of the experiment and enumeration.

Task 1.1 Growth of Aerobic Autotrophs

For this experiment, a bacterium belonging to the family *Nitrosomonadaceae* was used which are obligate aerobes, gram-negative, chemolitho-autotrophs. This means that they require oxygen, utilize the chemical oxidation of an inorganic nitrogen compound for their energy source, and require carbon dioxide as a carbon source (Reynolds and Richards, 1996). Of the ammonia-oxidizing *Nitrosomonadaceae* known, *Nitrosomonas* is the most common to be used in the lab and studied; however, *Nitrospira* is more

frequent in the environment (Hiorns et al., 1995). Therefore, the bacterium *Nitrosospira multiformis*, ATCC 25196, was selected as the organism of study. *Nitrosospira multiformis*, previously known as *Nitrosolobus multiformis*, was first isolated from soil samples obtained in various parts of the world in 1970 (Watson et al., 1971). Nonetheless, it has been found to be present in a wide variety of habitats, including marine, freshwater, sediments, and wastewater treatment facilities. It is a slow grower and has a doubling time of around 11 hours under optimum growth conditions.

Glycerol stock that was stored at -80°C was used as the source of *Nitrosospira multiformis*, ATCC 25196. The glycerol stock (4ml) was thawed on ice, inoculated into 36mL of pre-autoclaved medium (ATCC # 929), and incubated at 28°C in the dark. The media composition was ammonium sulfate 1.32 g, $\text{MgSO}_4 \cdot 7\text{H}_2\text{O}$ 380.0 mg, $\text{CaCl}_2 \cdot 2\text{H}_2\text{O}$ 20.0 mg, $\text{MnCl}_2 \cdot 4\text{H}_2\text{O}$ 200.0 μg , $\text{Na}_2\text{MoO}_4 \cdot 2\text{H}_2\text{O}$ 100.0 μg , $\text{CoCl}_2 \cdot 6\text{H}_2\text{O}$ 2.0 μg , $\text{ZnSO}_4 \cdot 7\text{H}_2\text{O}$ 100.0 μg , K_2HPO_4 87.0 mg, Phenol red 0.5% 0.25 ml, Chelated iron (Geigy Chem. 13% iron) 1.0 mg in 1.0 L Distilled water. Final pH was adjusted to 7.5 with 0.5 M K_2CO_3 and autoclaved at 121°C for 15 minutes. ATCC prescribed 929 medium contained $\text{NH}_3\text{-N}$, so the batch reactors were not supplemented with additional $\text{NH}_3\text{-N}$. Phenol red was added to the media in order to visually indicate the change in pH. As the bacteria consumes the bicarbonate supplied in the media, the pH decreases and the media changes from a reddish color to a yellow color. This change in color was also the visual indicator of bacterial growth. When the culture turned to the yellow color, it was inoculated into 10-fold additional media

for a progressive growth. At this point, whenever the culture turned to yellow color, NaCO_3 was added to maintain the pH levels at neutral and the culture was supplemental with fresh feed-stock. Since contamination is a common problem associated with the slow growing autotrophic bacteria, all the inoculations, samplings, and transfers were performed under a laminar-flow chamber and absolute sterile conditions were maintained. In cases of contamination, fresh subsamples were created from primary culture or glycerol stock.

The cultures were grown until visual turbidity was observed (around 10 days). After 10 days of growth, 1mL aliquots of the bacterial culture were collected. The samples were stained for 20 minutes in dark using 3 μL BacLight (Invitrogen, CA), collected onto a 0.22 μm filter (Millipore, CA) and mounted onto a clean glass slide (FisherBrand, PA). The slides were then checked under an epifluorescent microscope BX 51 microscope (Olympus, Japan) using Cy3 and FITC filters to capture pictures of live and dead cells, respectively. Micrographs obtained were used to ensure growth and to make sure there was no contamination. The experiment was started using a culture that had turned distinctly yellow, to ensure that there was no residual bicarbonate left in the system.

Task 1.2 Growth of Anaerobic Autotrophs

For the purpose of the second experiment, an autotrophic methanogen was used. *Methanobacterium subterraneum*, ATCC 700657, was one of the first autotrophic methane-producing archaea to be isolated from deep groundwater depths in 1996 (Kotelnikova et al., 1998). One of the isolates, denoted A8p (=DSM 11074T), was studied in detail; thus, it was selected for the experiment on

anaerobic autotrophic microbes. Under optimal conditions (20-40°C, pH 7.8-8.8, and 0.2-1.2 M NaCl), A8p has a doubling time of around 2.5 hours.

The autotrophic archaeon, *Methanobacterium subterraneum*, ATCC 700657, was obtained from ATCC, inoculated in autoclaved ATCC medium 1892 in serum vials, flushed with a gas mixture of 80% H₂, 20% CO₂, and incubated at 37°C in the dark. ATCC medium 1892 was prepared following the protocol prescribed. The medium contains resazurin that was used as a redox indicator. When redox potential is above -50 mV, it is pink, and colorless when the redox potential is below -110 mV. Most strict anaerobes require low redox potential (below -110 mv) for optimum growth. To keep the serum vials under positive pressure with anoxic head space, the serum bottles (75mL) were purged once every week with 80%(v/v) H₂, and 20%(v/v) CO₂ gas for 15 minutes.

Method Development

As the archaeon was growing, a few complications were encountered. The first problem occurred when the medium slowly began to turn pink as it sat in the serum vials. It was speculated that this indicated an introduction of oxygen into the system; however, there was no detected N₂/O₂ in head-space gas samples that were tested in a gas chromatograph (GC). As a counter measure to these complications, the bottles were purged more frequently. However, doing so caused further complications as a contaminant was introduced into the system, despite the stringent precautions taken. The type or source of the contamination was unclear. A fresh subculture was initiated using freshly prepared medium and the glycerol stock made from the primary culture.

In order to circumvent the leak problems, PTFE/Silicone septa (Thermo Scientific, PA) were used to seal the serum vials containing the cultures. These septa would prevent any leakage in or out of the bottles and maintain obligate anaerobic conditions.

Further, to get around the issue of contamination, a molecular probe (biomarker) was used which targeted the 16S-rRNA gene of *Methanobacterium subterraneum*. The probe MB1174 (Crocetti et al., 2006) specifically binds to the 16S rRNA gene of *Methanobacterium* and not to any other DNA from contaminant organism(s), thereby allowing selective enumeration of *Methanobacterium subterraneum*.

Genomic DNA was extracted from 2 to 3-days-old *Methanobacterium subterraneum* culture using a Ultraclean Soil DNA Isolation Kit (MO BIO Laboratories, Inc., CA) and following manufacturer's protocol. After extraction, the DNA quality was verified on 1% agarose gel. For 16S rDNA amplification, universal primers 8f and 1492r were used. The thermal cycle involved an initial denaturation at 95°C for 5 minutes, followed by 30 cycles of 1.5-minute denaturation at 95°C, 2 minutes of annealing at 52°C, and 3 minutes of extension at 72°C, with a final 10-minute extension at 72°C. The DNA quality and size of the amplicons was verified on 1% agarose gel and comparing with a 1kb DNA size ladder (Fermentas, CA). The amplicons were purified using QiaQuick Gel Extraction kit (QIAGEN Inc., CA) and DNA concentration was measured using Nanodrop. Based on the concentration measured and size of the amplicon (1487bp), copy number of 16S-rRNA genes in the stock was calculated. This

stock was serially diluted to obtain 10-fold concentration of 10^5 , 10^6 , 10^7 , 10^8 , 10^9 , 10^{10} , 10^{11} , 10^{12} , and 10^{13} . These stocks were used to obtain a standard curve and to quantify the cell-number of *Methanobacterium subterraneum* using quantitative PCR (qPCR) and MB1174 Taqman probe. RealplexS Mastercycler (Eppendorf, Germany) was used and the thermal cycle involved an initial denaturation at 95°C for 5 minutes, followed by 30 cycles of 1.5-minute denaturation at 95°C, 2 minutes of annealing at 52°C, and 3 minutes of extension at 72°C, with a final 10-minute extension at 72°C. In a final reaction volume of 20 μ L, 5-10 μ L culture as template was tested in triplicates.

The results from qPCR were inconclusive for quantification and conditions considered for probe-hybridization were speculated to be the possible reason. Due to this reason, enumeration based on flow-cytometry was chosen.

Task 2- Setup Experiment

Autotrophs are very slow growing because of the manner in which they must obtain energy. In order to study the autotrophs, it was necessary to isolate pure cultures in closed systems. The experiments were run over several consecutive days to determine a growth trend in batch reactors.

Task 2.1 Experimental Setup for Aerobic Autotrophs

Three batch reactors were set up in three 250 mL aspirator bottles at room temperature. Each aspirator was capped with a rubber cork containing 3x1/8th inch steel tubes connected to silicone tubing. Ends of each silicone tube were attached to 0.22 μ m filters to seal the bottles from the outside atmosphere, as

well as filter the incoming gas and feed. Experimental setup for a single batch reactor is depicted in Figure 3. The only difference between the three batch reactors was the amount of air and CO₂ gas entering the system and the incoming feed.

Bacterial culture (200mL) were transferred to each batch reactor and spiked with 50 mL of fresh ATCC medium 929 at $t=0$ to act as an ammonia supply for the bacteria. This volume of 250 mL was maintained throughout the experiment. Knowing the pH would drop, the reactors were started at a pH of 7.7 ± 0.2 and maintained at a pH of 7.3 ± 0.5 throughout the experiment. Two of the bottles were supplied with filtered air and CO₂ at a ratio 1:1 at low flows (approximately 1.5-3.0 mL/min), while the third was supplied with filtered air (without CO₂) at the same combined rate as the other two bottles. The bottle with just air pumped in and one of the batch reactors that was fed CO₂ and air were

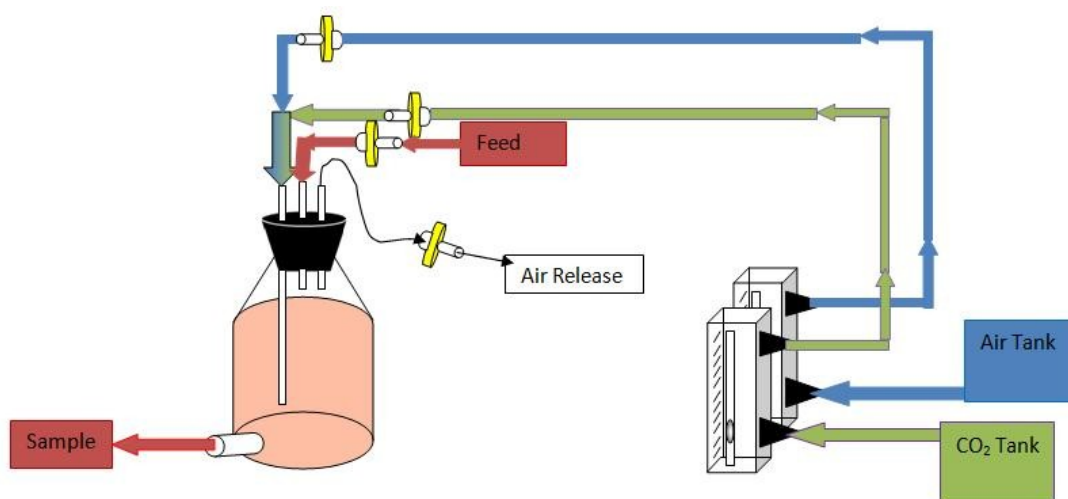


Figure 3- Batch reactor experimental setup for aerobic autotrophs

still fed with HCO_3 when the color indicator turned yellow. These batch reactors were used as controls. The third batch reactor was fed with CO_2 gas as the sole carbon source. Its pH was maintained by adding NaOH to the system whenever the color indicator turned yellow.

A sample of 3mL from each reactor was taken at $t=0$ hours and every 24 hours up to $t=96$ hours. From this 3mL sample, 1 mL was used at a 10% dilution to measure nutrients $\text{NH}_3\text{-N}$, $\text{NO}_3\text{-N}$, and $\text{NO}_2\text{-N}$. Another 1mL of the sample was used for bacterial enumeration using epifluorescent microscopy. The sample was stained for 20 minutes in the dark using 3 μl BacLight (Invitrogen, CA), collected onto a 0.22 μm filter (Millipore, CA) and mounted onto a clean glass slide (FisherBrand, PA). The slides were then checked under an epifluorescent BX 51 microscope (Olympus, Japan) using Cy3 and FITC filters to capture live and dead cells, respectively. Micrographs of random microscopic fields containing live (green stained) and dead (red stained) cells were captured. Number of live and dead cells in each micrograph was manually counted and was averaged. The percentage increase or decrease in the number of cells was calculated based on the average values. The last 1 mL of the sample was used to test the pH of the batch reactor using an automated pH controller.

Task 2.2 Experimental Setup for Anaerobic Autotrophs

Four batch reactors were set up in four 60 mL serum vials containing 20 mL of ATCC medium 1892 in each. Each vial was sealed with PTFE/Silicone septa (Fisherbrand, PA) and crimped with aluminum crimps. Each batch reactor was inoculated with 20 mL of pregrown *Methanobacterium subterraneum* using a

syringe and common source of culture. The vials were subsequently purged with 80% H₂ and 20% CO₂ v/v for 15 minutes to provide the same initial conditions. After incubation at 37°C for 4 hours, each vial was purged with varying amounts of gas concentrations to initialize the experiment. The first bottle was purged with 100% H₂ gas; every bottle thereafter was introduced to an increasing amount of CO₂ gas. The second bottle was purged with 90% H₂, 10% CO₂; the third with 80% H₂, 20% CO₂; the final bottle with 60% H₂, 40% CO₂. Following purging, the vials were incubated at 37°C. After 16 hours, 0.3 mL NaCO₃ was introduced into the first bottle to act as the carbon source. The experimental setup is depicted in Figure 4.

A sample of 3 mL from each reactor was taken at t=0 day and every day after for a total of 5 days. To keep the reactor in positive pressure and keep the gas in the appropriate concentrations, each bottle was purged for 15 minutes after the sample was taken. The 3 mL culture sample was centrifuged at 8000 x g for 30 minutes and the cell pellet was resuspended in 1 mL to concentrate the cells. This 1mL cell suspension was used for fluorescent in situ hybridization (FISH) with a MB1174 probe. Following FISH, 500 µL of the probe-hybridized sample was used for flow cytometry-based enumeration, while the other 500 µL

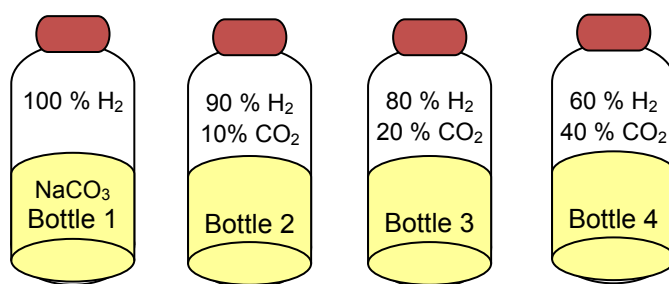


Figure 4- Experimental setup for anaerobic autotrophs

was viewed under the epifluorescent microscope. The pH was measured with the supernatant and maintained in the optimum range of 7.8 to 8.8. 1 N HCl was used to adjust the pH as needed.

Task 3- Quantify and Analyze Autotrophic Growth

There are several different methods that can be used to quantify the growth of the autotrophs. Aerobic autotrophs could be enumerated using stains and viewing under the microscope. Anaerobic autotrophs are different, seeing as they begin to die when exposed to oxygen. In order to enumerate the anaerobic, it needs to be fixed first to preserve the cell when exposed to air.

Task 3.1 Aerobic Autotrophic Quantification

Nutrient Detection and Quantification for Nitrifying Bacteria

The bacterial culture sample was diluted 10% to ensure the values were within detectable ranges. $\text{NH}_3\text{-N}$ was determined following standardized HACH method and using an AmVer High range Ammonia Reagent Set 26069-45. The absorbance was measured using a HACH spectrometer using a DR 5000. $\text{NO}_3\text{-N}$ and $\text{NO}_2\text{-N}$ are both inorganic anions and were determined by ion chromatography using a Metrohm 883 Basic IC Plus and an 863 Compact Auto Sampler. The remaining diluted sample was filtered through a $0.45\mu\text{m}$ filter and run through the IC following manufacturer's instructions.

Epifluorescence Microscopy and Bacterial Enumeration

A rapid epifluorescence staining method using the LIVE/DEAD Bacterial Viability Kit (*BacLight*) was applied to estimate total counts of the bacteria. The stain package is composed of a mixture of two nucleic acid-binding stains: SYTO9 and propidium iodide. SYTO9 stains all cells green while propidium iodide penetrates cells whose cell membrane has been damaged and stains them red (Boulos et. al., 1999). Samples were incubated in the dark for 20 minutes after an addition of 3 μ L of the dye. After incubation, the stained sample was filtered through a 0.2 μ m filter and the filter was mounted on a microscope slide under a drop of DABCO oil and a slide cover. Slides were analyzed under the microscope within 72 hours to avoid loss of fluorescence. A BX 51 microscope (Olympus, Japan) with Cy3 and FITC filters was used. Pictures were digitally captured at a magnification of 1000X with a DPI-71 camera. The bacteria were then enumerated manually using the Cell Counter plugin in ImageJ and based on the area of the filter.

Task 3.2 Anaerobic Autotrophic Quantification

Flow FISH Cell Fixation, Hybridization, and Archaea Enumeration

The sample (3 mL) taken from each anaerobic reactor was centrifuged at 8000 x g for 30 minutes to create a strong pellet. The pellet was resuspended and fixed using one part phosphate-buffered saline (PBS) solution (pH 7.2) and three parts of fresh (not older than 24 hours), cold 4% paraformaldehyde solution (4 g paraformaldehyde in 100 mL PBS, pH 7.2). The mixture was incubated at 4°C overnight. After fixing, the sample was centrifuged at 8,000 x g for 30

minutes, the supernatant was removed, and the pellet was washed in 1 mL of 1x PBS to remove residual fixative, and pelleted again. To create a 12.5 mM working stock solution, 100 μ L of 50 mM probe MB1174 was added to 900 μ L of 45% hybridization buffer (10 mL (3.6 N) NaCl, 0.8 mL Tris-HCL, 20 μ L 20% Sodium Dodecyl Sulfate, 11.18 mL deionized water, pH 7.2, 45% formamide). This mixture was added to the sample and was left to hybridize in a 46°C incubator overnight. From the hybridized sample, 500 μ L was immediately filtered with 0.22 μ m pore-sized-filters (Millipore, CA), mounted onto a gelatin coated slide, washed with 40% wash buffer (0.41 mL (3.6 N) NaCl, 0.8 mL Tris-HCL, 20 μ L 20% Sodium Dodecyl Sulfate, 38.77 mL deionized water, pH 7.2) for 20 minutes in 48°C, stained with 5 μ g/mL of 4', 6' -diamidino-2-phenylindole (DAPI) for 5 minutes, rinsed with cold, autoclaved, deionized water, and air-dried. The slides with cover glass were finally sealed with nail polish and stored at -20°C.

The other 500 μ L of the sample was stored at 4°C in the dark for no more than 1 week. This liquid sample was centrifuged at 8,000 x g for 30 minutes, and the supernatant was discarded. The pellet was resuspended in 500 μ L of a 40% wash buffer and incubated at 48°C for 20 minutes to remove all nonspecifically bound probes. Cells were finally pelleted at 8,000 x g for 30 minutes and suspended in 1 mL PBS with 5 μ L of DAPI and used for flow cytometry.

In order to determine the percentage of cells within the anaerobic batch reactors, a flow cytometer was used. A flow cytometer takes suspended cells in a stream of fluid and uses an electronic detection apparatus to scatter a beam of

light in order to detect fluctuations of brightness. Both Cy3-labelled probe and DAPI counter stain were used to ensure appropriate brightness and helped to selectively enumerate the target cells.

A flow cytometer, BDFACS Aria II, was used with a 405 nm (DAPI) and a 561 nm (Cy3) laser for 60 seconds at a slow, but varying speed. Approximately 50 μ L sample was used during that 60 seconds and the events (counted as cells) were enumerated based on Cy3 positive forward scatter.

CHAPTER 5

RESULTS AND DISCUSSION

Experiments with Aerobic Autotrophic Bacteria

Three batch reactors were tested to see if the nitrification capability was inhibited with the addition of CO₂. The first reactor was the reactor with no bicarbonate added and using CO₂ as the carbon source. NaOH was added to keep the pH steady. The second reactor was a control with bicarbonate and air but no CO₂. HCO₃ was added to keep the pH steady. The third reactor contained bicarbonate, air, and CO₂. HCO₃ was added to keep the pH steady.

The cells of *N. multiformis* that were examined under the epifluorescent microscope were spherical and measured at approximately 1.0µm in diameter. As they grew, the bacteria would clump together, making larger flocs or colonies. However, as the name indicates, the shape of the bacteria appeared in multiple forms, including elongated shapes. As seen in Figure 5, the backlight stained the live cells green and the dead cells red. The count of both live and dead cells was tabulated for each picture. Any cells that were a yellow color were considered dead.

Figure 6 shows the response of bacterial culture in the reactors. Panel A in Figure 6 shows cell counts in terms of dead, live, and total cell numbers in the batch reactor which received an inorganic carbon source in the form of CO₂ gas.

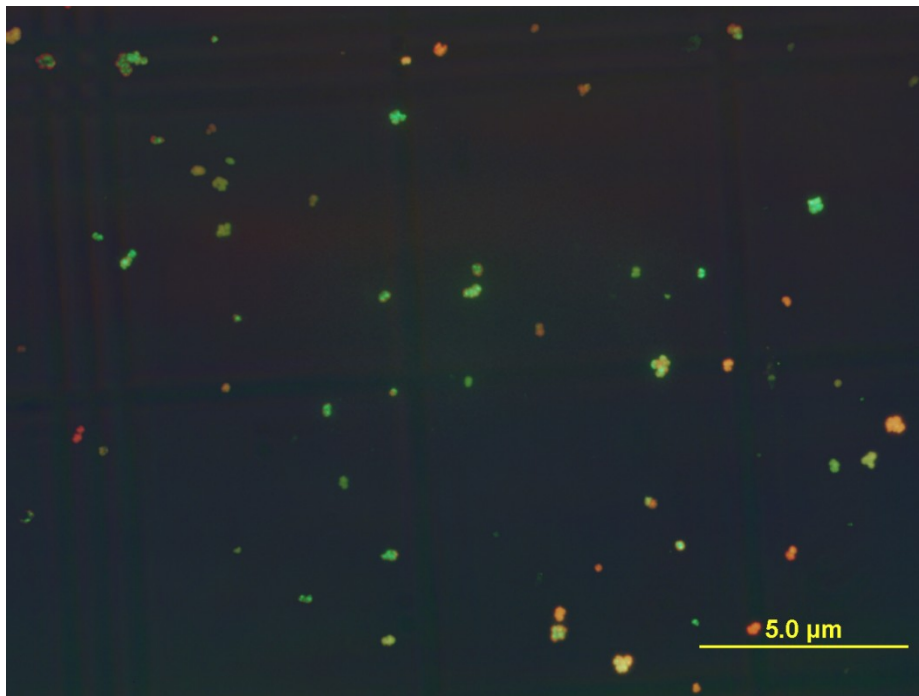


Figure 5- Epifluorescent *N. multiformis* stained with BacLight

Likewise, panel B in Figure 6 shows cell counts in terms of dead, live, and total cell numbers in the batch which received an inorganic carbon source in the form of bicarbonate. Panel C in Figure 6 received both carbon sources of CO₂ gas and bicarbonate.

It is quite evident from Figure 6, that the cell mixture which received bicarbonate as the inorganic carbon source shows faster and more consistent cell growth than the growth in the batch reactor which was maintained by bubbling CO₂. This is because bicarbonate is the preferred carbon source. CO₂ gas must be converted to bicarbonate before it can be utilized by the bacteria, which takes time and energy. However, the growth in panel A indicates that any existing bacteria in the system can utilize and be maintained by CO₂ as a carbon source. The growth in panel C suggests that an already growing system

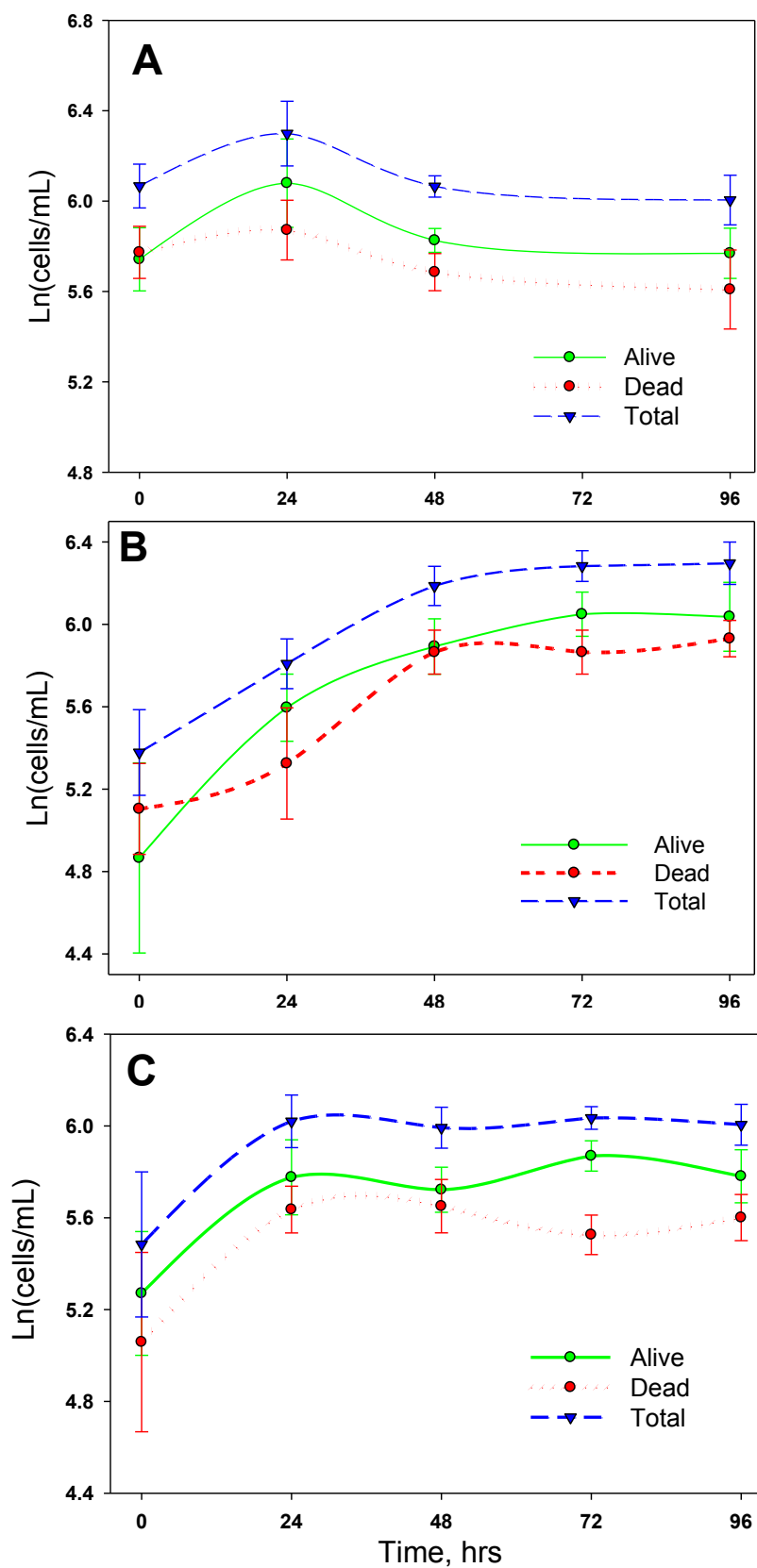


Figure 6- Cell counts in terms of dead, live, and total cell numbers for *N. Multiformis* which received inorganic carbon source in the form of A) CO₂ gas B) bicarbonate C) CO₂ gas and bicarbonate

supplied with bicarbonate is not hindered and may be slightly encouraged by extra CO₂ in the system. The specific growth rates were calculated for each reactor using the equation:

$$\mu = \frac{(X_{2L}-X_{1L})+(X_{2D}-X_{1D})}{X_{1T} \ 24 \ hr} \quad (18)$$

The specific growth rates that were calculated are given in Table 1 . The typical specific growth rates for Nitrosospira bacterium range from 0.018 to 0.070. Within these ranges, Nitrosospira is known to complete nitrification within wastewater treatment plants. The specific growth rates for all the reactors lie within these ranges, which means the growth of the bacteria is significant in all the tested conditions.

Nitrosospira multiformis is an ammonia oxidizer which converts ammonia nitrogen to nitrite by consuming the inorganic nitrogen source. Hence, the disappearance of ammonia nitrogen and the production of nitrite nitrogen was monitored to check if these biochemical reactions correlated with the growth rates. The changes are indicated in Figure 7.

Table 1-Specific growth rate for *N. Multiformis* batch reactors with different carbon sources

	Carbon source	Specific growth rate, μ (hr ⁻¹)
Reactor A	CO ₂ gas	0.032±0.006
Reactor B	Bicarbonate	0.063±0.012
Reactor C	Bicarbonate+CO ₂	0.071±0.016
Typical Nitrosospira range		0.018-0.070

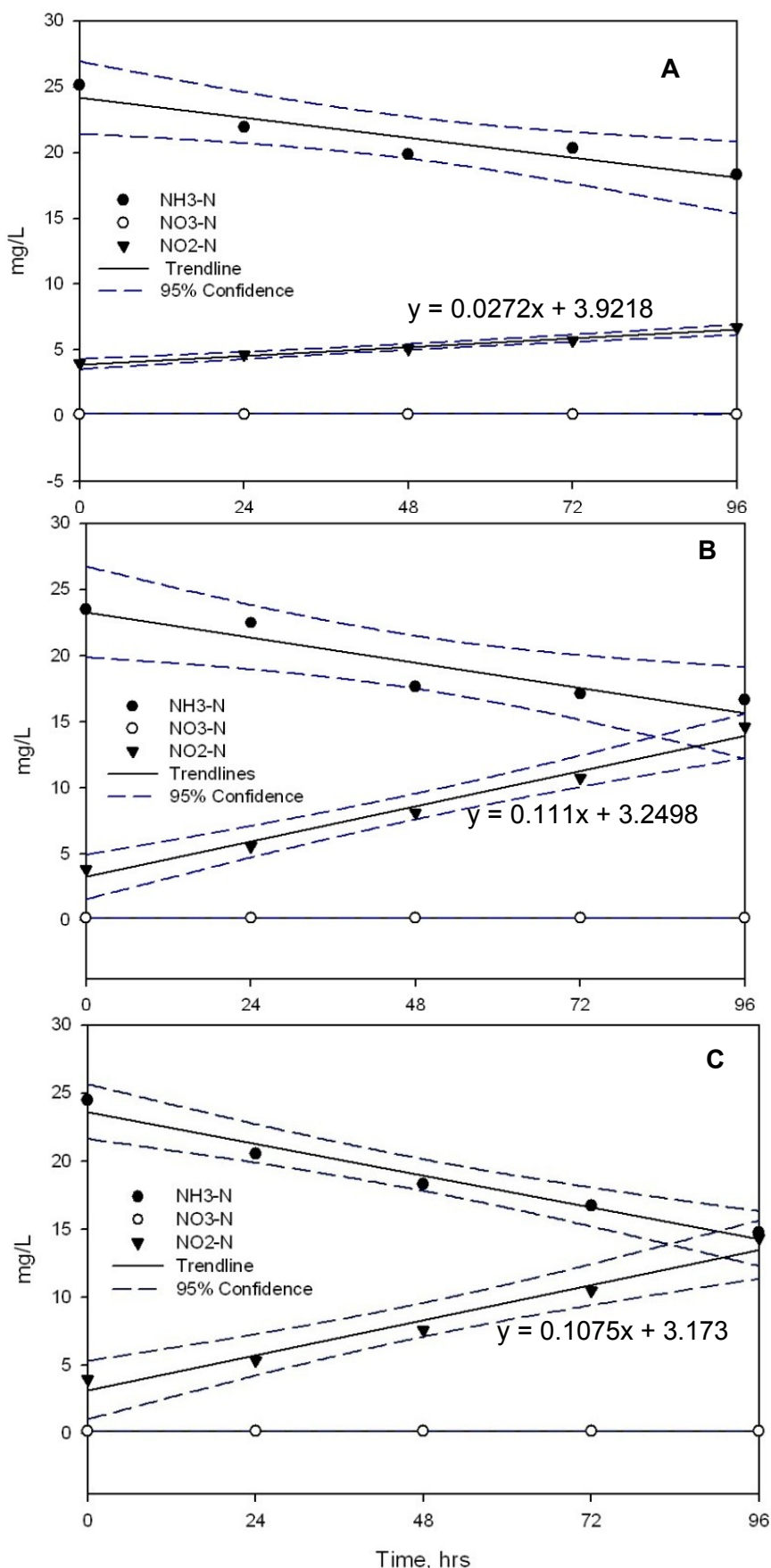


Figure 7- Partial nitrification performed by *N. multiformis* with inorganic carbon in the form of A) just CO₂ gas B) just bicarbonate C) both bicarbonate and CO₂ gas

As was expected, nitrate (indicated by white open circles) was not present or formed during the experiment. This is in agreement with the type of bacteria that was present, which converts ammonia to nitrite ($\text{NH}_3\text{-N} \rightarrow \text{NO}_2\text{-N}$) and does not complete nitrification to nitrate ($\text{NO}_2\text{-N} \rightarrow \text{NO}_3\text{-N}$). The three batch reactors started with 24.4 ± 0.8 mg/L of ammonia, $\text{NH}_3\text{-N}$. In panel A from Figure 7, the batch reactor which received an inorganic carbon in the form of CO_2 , $\text{NH}_3\text{-N}$ decreased from 25.1 mg/L to a value of 18.3 mg/L. The rate of nitrite production ($\text{NH}_3\text{-N} \rightarrow \text{NO}_2\text{-N}$) was 0.0272 mg $\text{NO}_2\text{-N/L-hr}$. The reactor with just bicarbonate, seen in panel B from Figure 7, decreased from 23.5 to 16.7 mg/L and the reactor with both bicarbonate and CO_2 gas, seen in panel C from Figure 7, reduced from 24.5 to 14.7 mg/L. However, the rate of nitrite from the batches which were fed bicarbonate, seen in panels B and C, were approximately 0.11 mg $\text{NO}_2\text{-N/L-hr}$. This is almost five times more than the rate in the first reactor fed with CO_2 gas.

These results correspond well with the results from the growth curves shown in Figure 6. The low growth in the batch reactor with CO_2 as the carbon source show low nitrite production. But the nitrite data collected show that the bacteria is still working and growing under those conditions, just at a slower rate. Panels B and C in Figure 7 support the growth seen in Figure 6 and support the conclusion that nitrite production is not affected with additional CO_2 in the system.

Experiments with Anaerobic Autotrophic Archaea

Four batch reactors were set up and tested to determine that the growth rate of anaerobic archaeon was affected by varying amounts of CO_2 , as seen in

Table 2. The first reactor had an atmosphere of 100% hydrogen gas and bicarbonate in the media as a carbon source to determine the effect of dissolved CO₂ in the system. The second reactor contained a carbon dioxide limiting atmosphere of 90% H₂+10% CO₂ v/v. The third reactor had a 80% H₂+20% CO₂ v/v atmosphere, which was the recommended optimum growth conditions for this methanogen. The fourth reactor had an atmosphere of 60% H₂ and 40% CO₂, which provided the conditions for excess CO₂.

A sample was taken from each reactor, and submitted to Cy3 probe and DAPI staining. Half was viewed under an epifluorescent microscope and the other put through a flow cytometer. When viewed under a microscope, the *M. subterraneum* was seen as small, thin, slightly curved rods approximately 1µm in length. They grew either individually or in large clumps.

The MB1174 probe was able to bind to the fixed cells. However, not all of the observed cells were illuminated, even when fixed for longer periods of time.

This problem occurred, especially when there were large clumps of cells. Figure 8 shows this when the cells illuminated by the probe (top) are compared

Table 2-Growth conditions for anaerobic archaea

	Atmosphere (% v/v)	Carbon source
Reactor 1	100% H ₂	Bicarbonate only
Reactor 2	90% H ₂ +10% CO ₂	Bicarbonate+CO ₂
Reactor 3	80% H ₂ +20% CO ₂	Bicarbonate+CO ₂
Reactor 4	60% H ₂ +40% CO ₂	Bicarbonate+CO ₂

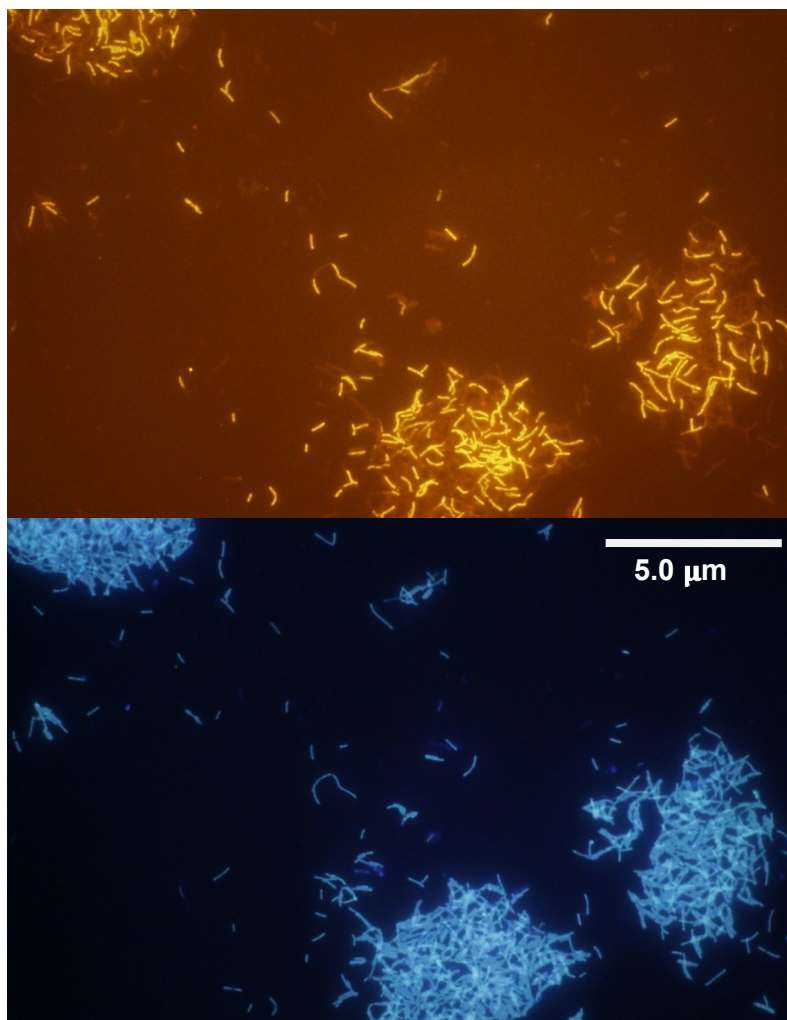


Figure 8- *M. Subterraneum* viewed under epifluorescent microscopy comparing a Cy3 probe (top) to DAPI staining (bottom)

to the same cells illuminated by DAPI (bottom). The probe was used to negate any contamination, but no apparent contamination was visible under the microscope.

Two times diluted samples from 5 consecutive days were sent through a flow cytometer. The forward scatter was compared for each reactor at each day. The cells were enumerated from particle overlay of DAPI and probe counts for reactor 1 can be seen in Figure 9, which acts as an example for all 5 days.

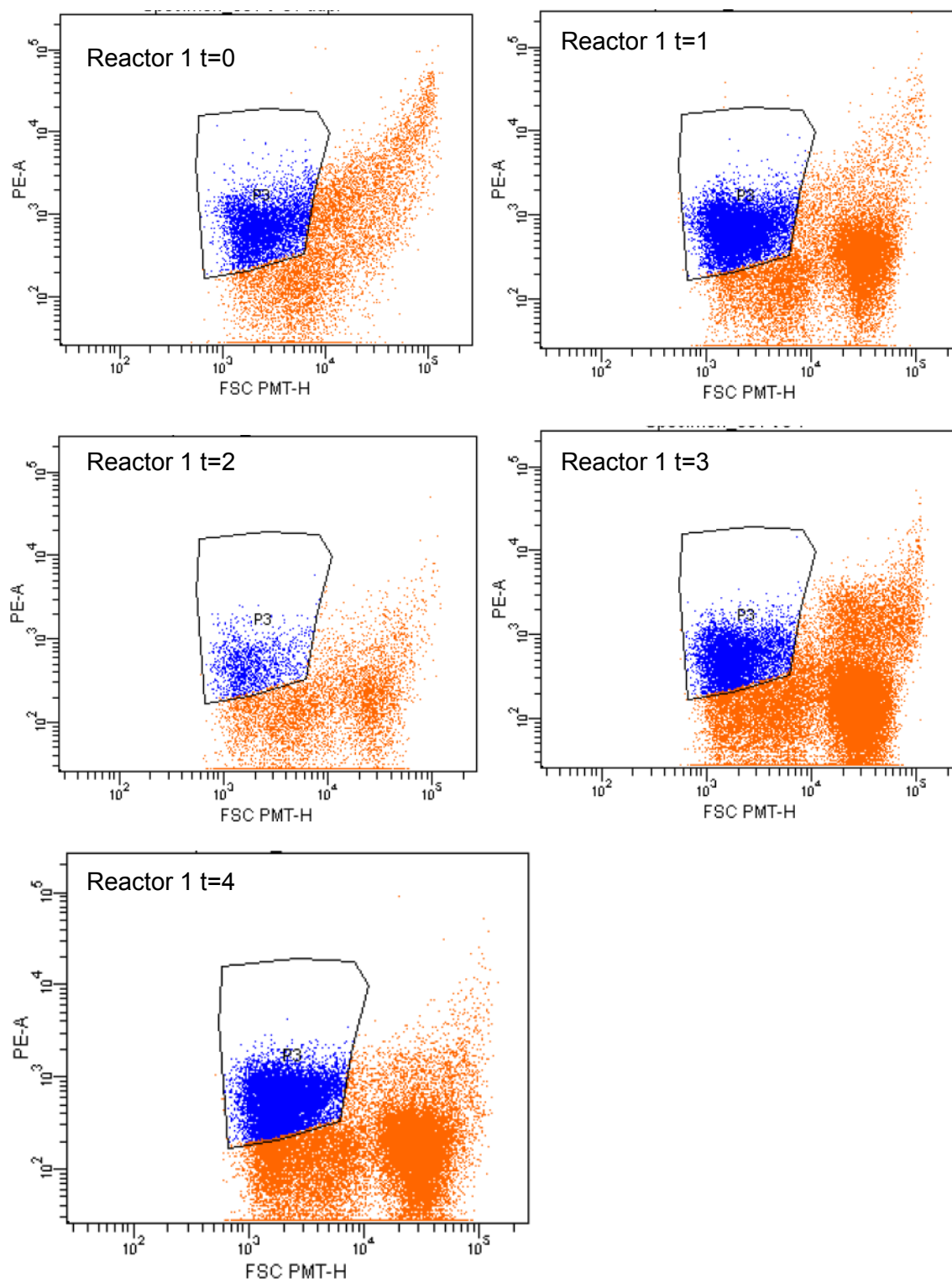


Figure 9- Flow cytometry forward scatter for reactor 1

Reactor 1 was interesting because of a distinct extra grouping of particles which were not accounted for and not found in any other reactor. The particles that were considered cells were isolated in a gate and enumerated. These enumerated values were plotted according to time with reference to each reactor, as seen in Figure 10.

According to Figure 10, the reactor that uses bicarbonate as a carbon source remained approximately steady, while the other three bottles had stimulated growth with an excess of carbon dioxide. Disregarding the data points on day 4, Reactor 4 had a growth rate of 9500 cells/day over 3 days; reactor 3 had a growth rate of 7800 cells/day; and reactor 2 had a growth rate of 6800 cells/day. The trends from the plot show that with a consistent amount of H_2 , an addition of CO_2 caused a greater growth rate over the 3 days.

When collecting the samples for day 2, all of the samples that were

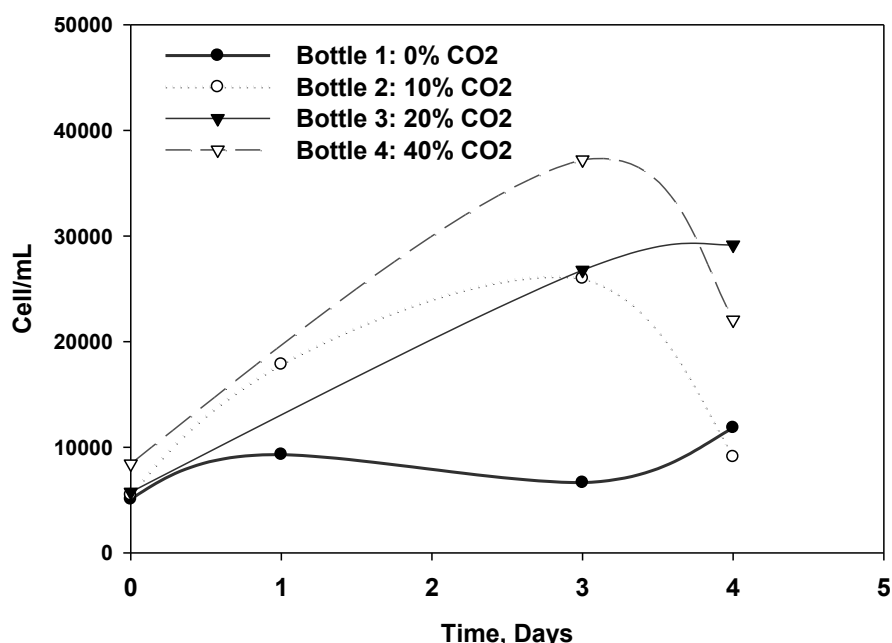


Figure 10- Enumerated cells through flow cytometry

extremely low were enumerated and the data were not included. For day 1, the sample vials for reactor 3 and 4 had cracks so the pellets were lost in the centrifuge, meaning these two data points were not included in the analysis. Because of the inaccuracies in the sampling, it was unclear which conclusions to make and the experiment was repeated for further analysis.

Repeated Experiment

The second run through the experiment was conducted according to the same protocol as the first run through. The only differences were that no additional bicarbonate was given to the control bottle, and the whole experiment was run 1 additional day. The events were enumerated using the flow cytometry by the specialist running the machine. Two runs for each sample were conducted and the average for each was taken. The events were adjusted according to dilution to enumerate as counts per mL. Two different counts were

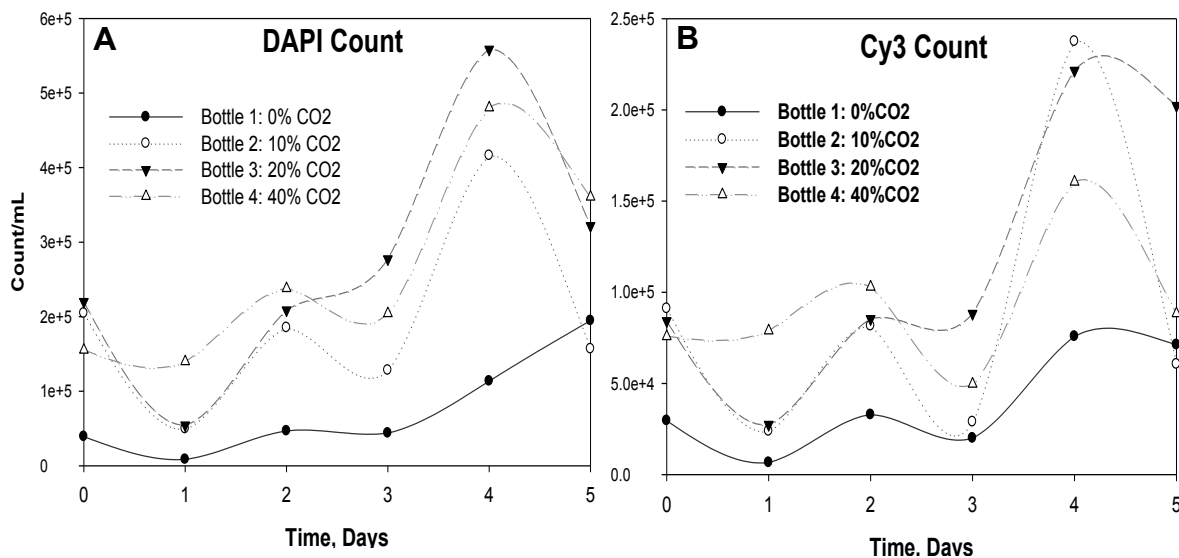


Figure 11- Flow cytometry enumeration for *M. Subterraneum* stained by A) DAPI and B) Cy3 probe

achieved from the flow cytometry. One was the events stained by DAPI which stains all DNA (Figure 11 panel A). The other was the fluorescence from the Cy3 probe, (Figure 11 panel B).

Ideally, in a pure culture, these two numbers would be the same. The experiment resulted in numbers that Cy3 was approximately half of the DAPI count and gave slightly different trends. The DAPI had a steadier climb, indicating bottle 3 and 4 had the best growth, while the Cy3 was inconsistent, but indicated bottle 2 and 3 had the best growth.

To normalize the counts, the cell count was divided by the initial concentration for the individual bottles. From the plot from the normalized events stained with DAPI, seen in Figure 12 panel A, the bottle with the excess carbon dioxide has a greater growth rate than the rest of the bottles. However, the bottle with the bicarbonate had a slow start but then continued at a rapid speed through day 5.

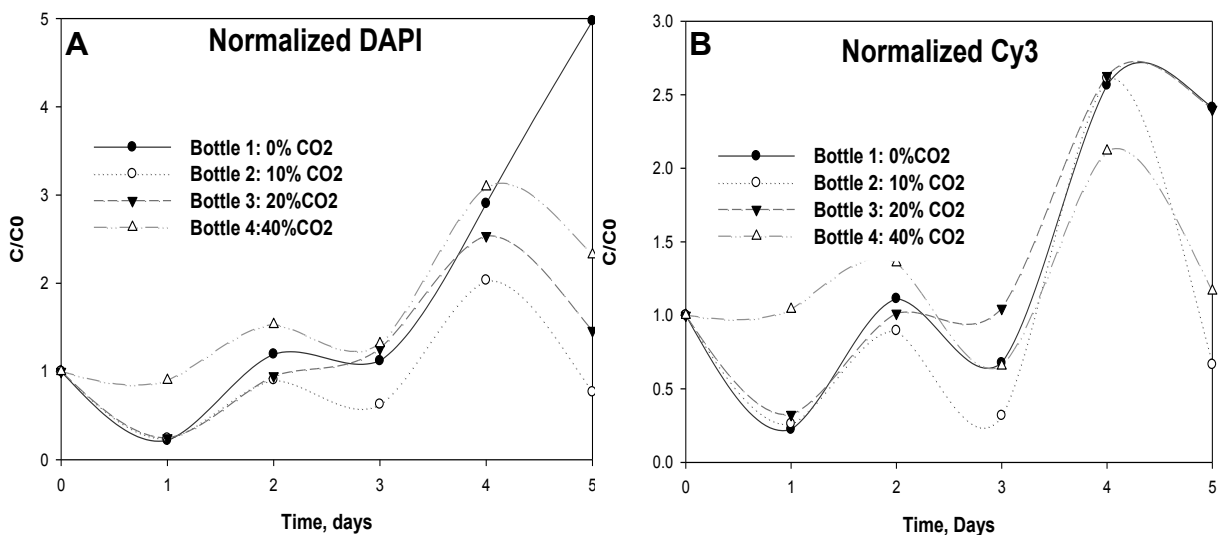


Figure 12- Enumeration of *M. subterraneum* stained with A) DAPI and B) Cy3 probe normalized based on initial concentrations

Since the trends differ depending on whether the DAPI or Cy3 data are analyzed, it is unclear which gives a more accurate depiction of the growth rate of the bacteria. The DAPI emits more fluorescence and would give a clearer reading; however cell count would include any contamination within the system. The Cy3 is specific to the archaeon that was being looked at, however, when looked at under the microscope, it was determined that the probe was having difficulty fully binding to all of the cells. This meant that many of the cells while passing through the flow cytometry could not be distinguished from the background.

On both accounts, day 5 led to a drop in the cell count. This may be because the micronutrients in the medium had been depleted and not been replaced. This would explain the reason why bottle 1 still grew on day 5, since the original concentration of cells was fewer than the other bottles and thus had not fully used all of the nutrients by day 5.

The results from this experiment were not very conclusive, but are encouraging for future research. By further optimizing this protocol, the results can be fine tuned to achieve more accurate results.

CHAPTER 6

CONCLUSIONS

Carbon dioxide sequestration with deep saline injection has the potential to help mitigate the green house effect enhanced by the increasing carbon dioxide concentration in the atmosphere. However, long-term storage of carbon dioxide raises concerns about the effect on geochemistry and subsurface microbiology if it were to leak. The experiments conducted towards this thesis studied the effect of carbon dioxide on the growth of two different microorganisms that are known subsurface inhabitants. The following conclusions can be drawn from my research and literature studied.

1. Geological sequestration of CO₂ is an excellent option as highlighted in several publications but the possibility of groundwater contamination should be considered.
2. Both aerobic and anaerobic autotrophic growths were found to be supported by carbon dioxide gas.
3. The aerobic autotrophic bacterium, *Nitrosospria multiformis* at 23°C, pH of 7.3 ± 0.5, 1.5-3.0 mL Air+CO₂/minute was able to maintain growth and nitrification. There was more bacterial growth when supplied with bicarbonate as a carbon source and the CO₂ had no inhibitory effects. However, experiments were done under one experimental condition and more experiments, including variability in system pH, variable pressure,

- and inhibitors such as heavy metals or other geochemical minerals should be conducted.
4. The anaerobic archaeon, *Methanobacterium subterraneum* at 37°C, pH of 8.3± 0.5, grew on strictly bicarbonate, but the addition of CO₂ gas stimulated the growth of the autotrophs until the micronutrients in the system were depleted. However, due to challenges with contamination and probe hybridization, the effective growth rate was unclear. It seemed the archaeon could adapt to using bicarbonate as its only carbon source and it is unclear how its growth would have been affected if the experiment were to continue for longer. Optimization of the probe use and this protocol would give more accurate results.
 5. Since little research has been conducted on the effect of geologic carbon sequestration on deep subsurface microbiology, this research laid down an important foundation for future research.

REFERENCES

Bachu, S.; Adams, J. J. Sequestration of CO₂ in geological media in response to climate change: capacity of deep saline aquifers to sequester CO₂ in solution. *Energy Conversion and Management* **2003**, *44* (20), 3151-3175.

Benson, S. M.; Cloe, D. R. CO₂ Sequestration in Deep Sedimentary Formations. *GS Elements* **2008**, *4*, 325-331.

Benson, S.M.; Hepple, R., Apps, J.; Tsang, C. F.; Lippmann, M. *Lessons Learned from Natural and Industrial Analogues for Storage of Carbon Dioxide in Deep Geological Formations*; Report LBNL- 51170; Lawrence Berkeley National Laboratory, Berkeley, CA, 2002.

Caron, F.; Manni, G.; Workman, W. J. A large-scale laboratory experiment to determine the mass transfer of CO₂ from a sandy soil to moving groundwater. *Journal of Geochemical Exploration* **1998**, *64*, 111-125.

Cole, J. J.; Prairie, Y. T. Dissolved CO₂, G. E. Likens, ed.; *Encyclopedia of Inland Waters* **2009**, *2*, 30-34.

Crocetti, G.; Murto, M.; Björnsson, L. An update and optimization of oligonucleotide probes targeting methanogenic Archaea for use in fluorescence in situ hybridization (FISH). *Journal of Microbial Methods* **2006**, *65*, 194-201.

Damen, K.; Faaij, A.; Turkenburg, W. *Health, Safety, and Environmental Risks of Underground CO₂ Storage: Overview of Mechanisms and Current Knowledge*; Copernicus Institute for Sustainable Development and Innovation, Department of Science, Technology and Society. Heidelberglaan: Springer, 2006.

Hansel, C. M.; Fendorf, S.; Jardine, P. M.; Francis, C. A. Changes in Bacterial and Archaeal Community Structure and Functional Diversity along a Geochemically Variable Soil Profile. *Applied and Environmental Microbiology* **2008**, *74* (5), 1620-1633.

Hiorns, W. D.; Hastings, R. C.; Head, I. M.; McCarthy, A. J.; Saunders, J. R.; Pickup, R. W.; Hall, G. H. Amplification of 16s ribosomal RNA genes of autotrophic ammonia-oxidizing bacteria demonstrates the ubiquity of nitrospiras in the environment. *Microbiology* **1995**, *141*, 2793-2800.

IPCC. *IPCC Special Report: Carbon Dioxide Capture and Storage. Summary for Policy Makers and Technical Summary*; B. Metz, O. Davidson, H. de Coninck, M. Loos, and L. Meyer eds.; Cambridge University Press, New York, 2005.

Kotelnikova, S. Microbial production and oxidation of methane in deep subsurface. *Earth-Science Reviews* **2002**, *58*, 367-395.

Kotelnikova, S.; Macario, A.; Pedersen, K. *Methanobacterium subterraneum* sp. nov., a new alkaliphilic, eurythermic and halotolerant mathanogen isolated from deep granitic groundwater. *Int J Syst Bacteriol* **1998**, *48*, 357-367.

LaGrega, M. D.; Buckingham, P. L.; Evans, J. C. *Hazardous Waste Management*, Second 162-212 ed. Long Grove, IL: Waveland Press, Inc, 2010.

Metcalf & Eddy, Inc. *Wastewater Engineering: Treatment and Reuse*, 4th ed.; New York, NY: McGraw-Hill Companies, Inc, 2003.

NETL: Carbon Sequestration Atlas of the United States and Canada, 2007; Appendix A: Methodology for Development of Carbon Sequestration Capacity Estimates.

Onstott, T. C. Impact of CO₂ Injections on Deep Subsurvace Microbial Ecosystems and Potential Ramifications for the Surface Biosphere. *Carbon Dioxide Capture for Storage in Deep Geologic Fromations* **2005**, *2*, 1217-1249.

Saripalli, K. P.; Cook, E. M.; Mahasanen, N. 2002. Risk and hazard assessment for projects involving the geological sequestration of CO₂, In *Proceedings from 6th International Conference on Greenhouse Gas Technologies*; Gale, J. and Kaya, Y. eds.; Kyoto, 2002.

Shuler, M. L.; Kargi, F. *Bioprocess Engineering: Basic Concepts*, 2nd ed.; Upper Saddle River, NJ: Pearson Education, Inc, 2002.

Stumm, W.; Morgan, J. J. *Aquatic Chemistry: Chemical Equilibria and Rates in Natural Waters*, 3rd ed.; New York, NY: John Wiley & Sons, Inc, 1995.

Turley, C.; Blackford, J. C.; Widdicombe, S.; Lowe, D.; Nightingale, P. D.; Rees, A. P. Reviewing the impact of increased atmospheric CO₂ on oceanic pH and the marine ecosystem. *Avoiding Dangerous Climate Change*; H.J. Schellnhuber ed.; Cambridge University Press, Cambridge, UK, 2006, 65-70.

U.S. Environmental Protection Agency. Vulnerability Evaluation Framework for Geologic Sequestration of Carbon Dioxide, 2008.

Wang, S.; Jaffe, P. R. Dissolution of a mineral phase in potable aquifers due to CO₂ releases from deep formations; effect of dissolution kinetics. *Energy Conversion and Management* **2004**, *45*, 2833-2848.

Watson, S. W.; Graham, L. B.; Remsen, C. C.; Valois, F. W. A Lobular, Ammonia-Oxidizing Bacterium, *Nitrosolobus multiformis* Nov. Gen. Nov. Sp. *Arch. Mikrobiol* **1971**, *76*, 183-203.

Zheng, C.; Bennet, G. D. *Applied Contaminant Transport Modeling*. New York, NY: International Thomson Publising Inc, 1995.